Prediction of Turbulent Heat Transfer in Swirling Flow Downstream of an Abrupt Pipe Expansion

Kwang-Yong Kim* and Yoon-Seok Chang*

(*Received October 9, 1996*)

Turbulent heat transfer characteristics in swirling flows downstream of an abrupt pipe expansion with a diameter ratio of 0.5 are predicted by full Reynolds stress model. The uniform heat flux condition is imposed on the downstream wall. The flows with weak and strong swirls as well as without swirl are computed. The governing differential equations are discretized by finite volume method. Results show that the Reynolds stress model predicts accurately the maximum local Nusselt number for the case with strong swirl, but that the effects of swirl are not fully accounted for the case with weak swirl.

Key Words: Turbulent Heat Transfer, Swirling Flow, Abrupt Pipe Expansion, Reynolds Stress Model, Finite Volume Method

Nomenclature

c_p : Constant pressure specific heat, $J/kg\cdot℃$
D : Diameter of a large pipe
k : Turbulent kinetic energy or thermal conductivity
Nu : Nusselt number ($=q''D/k(T_w-T_b)$)
p : Pressure fluctuation
P : Mean pressure or production rate of k
Pr : Prandtl number
q''_w : Wall heat flux, $J/m^2\cdot s$
R : Radius of a large pipe
Re : Reynolds number
S : Swirl number
T : Mean temperature
T_b : Bulk temperature
U, V, W : Mean velocities in x, r and θ directions, respectively
$\overline{u_iu_j}$: Reynolds stress
$\overline{u_i\theta}$: Turbulent thermal flux
x, r : Axial and radial coordinates, respectively
α : Thermal diffusivity, m^2/s
δ_{ij} : Kronecker delta
ε : Dissipation rate of k
θ : Temperature fluctuation
μ, ν : Dynamic and kinematic viscosities, respectively
ρ : Fluid density, Kg/m^3
τ : Shear stress

Subscripts

n : Direction normal to a wall
p : Value at the node adjacent to a wall
w : Wall value

* Department of Mechanical Engineering, INHA University, Incheon, KOREA

1. Introduction

Swirling turbulent flow downstream of an abrupt pipe expansion has a very complex flow structure such that recirculation of the flow due to the separation is superposed on the swirl. Both swirl and recirculation enhance the heat transfer coefficient several times greater than that for the fully developed turbulent pipe flow at the same Reynolds number, which is mainly attributed to the increase in turbulent kinetic energy due to the large curvature of streamlines. For this reason, applications of this flow to the heat exchangers or to the combustion chambers are effective to enhance the heat and mass transfers.

One of the interesting features of the strongly

swirling flow is the formation of recirculation zone near the central axis. Decay of tangential velocity components results in an increase in static pressure near the axis. And, the consequent adverse pressure gradient on the central axis may drive the recirculation when the swirl number is sufficiently high. The other important phenomena found in experiments on swriling flow is the existence of an unsteady asymmetry, which depends on flow geometry and swirl number.

Flowfield downstream of a sudden expansion consists of a free shear layer, a recirculation zone due to the separation, a reattachment zone, and a redevelopment zone. In the free shear layer, high level of turbulent kinetic energy is generated by shearing as the jet issues into the larger pipe. The turbulent kinetic energy generated in this shear layer dissipates relatively slowly since the dissipation rates are relatively low in this layer away from the wall. The high level of turbulent kinetic energy increases the turbulent diffusion, reduces the thickness of the viscous sublayer, and thus increases the heat transfer rate at the wall.

When the swirl is imposed on the flow through a sudden expansion, turbulent kinetic energy increases by the effects of streamline curvature, and the length of the wall-bounded recirculation zone decreases by the effects of centrifugal force. In addition, swirl may cause the recirculation around the axis and unsteady asymmetries mentioned above.

The effects of the swirl and separation due to the sudden enlargement of the flow in a pipe usually have been studied individually so far. And, the investigations on swirling flow through a sudden expansion have been limited by the complexity of the flow.

Lilley and his collegues reported a series of experimental work (Jackson and Lilley, 1983; Rhode, et al., 1983; Yoon and Lilley, 1984) on this flow. However, on the heat transfer characteristics, we could find only the work of Dellenback et al. (1987). They reported the measurements on velocity and heat transfer characteristics of this flow with 2 : 1 expansion and uniform wall heat flux boundary condition. In this experiment, swirl number was varied from zero to 1.2, and the Reynolds number from 30,000 to 100,000. And, they found that the maximum Nusselt number has the values from 3 to 9.5 times larger than those for the fully developed pipe flow, and that location of the maximum heat transfer occures upstream of the flow reattachment point. The unsteady asymmetry was found only at the lowest nonzero swirl number.

There have been several computational investigations (Prud'homme and Elghobashi, 1986; Kim and Lee, 1994) on the heat transfer for the flow through a sudden expansion. Among these, Kim and Lee (1994) reported the computational results with a second-order turbulence closure, which are much better than those with $k-\varepsilon$ model in the predictions of velocity and temperature fields as well as the heat transfer coefficients. For this flow with swirl, Habib and McEligot (1982) calculated the heat transfer rates with a conventional $k-\varepsilon$ model, which were not validated by any reliable experimental data. Sultanian (1984) reported on the calculations with algebraic stress model which is a simplified version of second-order closure. They did not, however, include the heat transfer calculations.

In the present work, numerical predictions with a second-order turbulence closure have been obtained for the convective heat transfer in the swirling turbulent flow downstream of a sudden expansion in a pipe. The results on the mean flow and heat transfer characteristics are discussed in comparison with experimental data of Dellenback (1986).

2. Turbulence Closures

Since the unsteady asymmetry does not occur in strongly swirling flows, we have assumed that the flows are steady and axisymmetric. The Reynolds -averaged Navier-Stokes equations and the energy equation for the steady, incompressible, axisymmetric, turbulent flow are written in cylindrical coordinates as follows.

$$\rho U\frac{\partial U}{\partial x}+\rho V\frac{\partial U}{\partial r}=-\frac{\partial}{\partial x}\left[\mu\frac{\partial U}{\partial x}-\overline{\rho u^2}\right]+\frac{1}{r}\frac{\partial}{\partial r}\left[r\left(\mu\frac{\partial U}{\partial r}-\rho\overline{uv}\right)\right]-\frac{\partial P}{\partial x} \quad (1)$$

$$\rho U\frac{\partial V}{\partial x}+\rho V\frac{\partial V}{\partial r}=\frac{\partial}{\partial x}\left[\mu\frac{\partial V}{\partial x}-\rho\overline{uv}\right]+\frac{1}{r}\frac{\partial}{\partial r}\left[r\left(\mu\frac{\partial V}{\partial r}-\rho\overline{v^2}\right)\right]-\mu\frac{V}{r^2}+\rho\frac{\overline{w^2}}{r}-\frac{\partial P}{\partial r} \tag{2}$$

$$\rho U\frac{\partial(rW)}{\partial x}+\rho V\frac{\partial(rW)}{\partial r}=\frac{\partial}{\partial x}\left[\mu\frac{\partial(rW)}{\partial x}-r\rho\overline{uw}\right]+\frac{1}{r}\frac{\partial}{\partial r}\left[r\left(\mu\frac{\partial(rW)}{\partial r}-r\rho\overline{uw}\right)\right]-2\mu\frac{W}{r}-2\mu\frac{\partial W}{\partial r} \tag{3}$$

$$\rho U\frac{\partial T}{\partial x}+\rho V\frac{\partial T}{\partial r}=\frac{\partial}{\partial x}\left[\frac{\mu}{Pr}\frac{\partial T}{\partial x}-\rho\overline{u\theta}\right]+\frac{1}{r}\frac{\partial}{\partial r}\left[r\left(\frac{\mu}{Pr}\frac{\partial T}{\partial r}-\rho\overline{v\theta}\right)\right] \tag{4}$$

Reynolds stress model as a second-order closure solves the transport equations for the Reynolds stresses and the turbulent thermal fluxes. The transport equation for the Reynolds stress tensor can be written as

$$\frac{\partial}{\partial x_k}(U_k\overline{u_iu_j})=D_{ij}+P_{ij}+\Phi_{ij}-\varepsilon_{ij} \tag{5}$$

where,

$$D_{ij}=-\frac{\partial}{\partial x_k}(\overline{u_iu_ju_k})$$

$$P_{ij}=-\left[\overline{u_ju_k}\frac{\partial U_i}{\partial x_k}+\overline{u_iu_k}\frac{\partial U_j}{\partial x_k}\right]$$

$$\Phi_{ij}=\overline{\frac{p}{\rho}\left[\frac{\partial u_i}{\partial x_j}+\frac{\partial u_j}{\partial x_i}\right]}$$

$$\varepsilon_{ij}=2\nu\overline{\frac{\partial u_i}{\partial x_k}\frac{\partial u_j}{\partial x_k}}$$

For the turbulent diffusion term, D_{ij}, Daly and Harlow's simple gradient diffusion model (1970) is used in this work.

$$D_{ij}=\frac{\partial}{\partial x_k}\left[c_s\frac{k}{\varepsilon}\overline{u_ku_l}\frac{\partial\overline{u_iu_j}}{\partial x_l}\right] \tag{6}$$

By the assumption of local isotropy of the smallest eddies, following isotropic model for the dissipation rate, ε_{ij}, is employed.

$$\varepsilon_{ij}=\frac{2}{3}\varepsilon\delta_{ij} \tag{7}$$

The pressure-strain rate interaction term, Φ_{ij}, reflects the return-to-isotropy characteristics of turbulent motion. The Poisson equation for the pressure fluctuation indicates that there are two different kinds of interactions: one by turbulent motion ($\Phi_{ij,1}$) and the other by mean motion ($\Phi_{ij,2}$), and also that there is an effect of solid wall boundary ($\Phi_{ij,w}$).

$$\Phi_{ij}=\Phi_{ij,1}+\Phi_{ij,2}+\Phi_{ij,w} \tag{8}$$

For the interaction term by turbulence, following Rotta's proposal (1951) is widely used in second-order closures.

$$\Phi_{ij,1}=-c_1\frac{\varepsilon}{k}\left(\overline{u_iu_j}-\frac{2}{3}\delta_{ij}k\right) \tag{9}$$

As a model for the interaction term by mean motion, the simplified version of the model proposed by Launder et al. (1975) is empolyed in this work.

$$\Phi_{ij,2}=-c_2\left(P_{ij}-\frac{2}{3}\delta_{ij}P\right) \tag{10}$$

where P is a production rate of turbulent kinetic energy. As proposed by Gibson and Launder (1978), the following model is adopted for wall reflection term.

$$\Phi_{ij,w}=c_1'\frac{\varepsilon}{k}\left(\overline{u_n^2}\delta_{ij}-\frac{3}{2}\overline{u_nu_i}\delta_{nj}-\frac{3}{2}\overline{u_nu_j}\delta_{ni}\right)f+c_2'\left(\Phi_{nn,2}\delta_{ij}-\frac{3}{2}\Phi_{ni,2}\delta_{nj}-\frac{3}{2}\Phi_{nj,2}\delta_{ni}\right)f \tag{11}$$

where f is a wall damping function defined by

$$f=\frac{c_\mu^{3/4}k^{3/2}}{\varkappa}(R-r)\varepsilon \tag{12}$$

The equation for the dissipation rate of turbulent kinetic energy used in this work is the same as that proposed by Launder et al. (1975) as follows.

$$U_k\frac{\partial\varepsilon}{\partial x_k}=\frac{\partial}{\partial x_k}\left[c_\varepsilon\frac{k}{\varepsilon}\overline{u_ku_l}\frac{\partial\varepsilon}{\partial x_l}\right]+c_{\varepsilon1}\frac{\varepsilon}{k}P-c_{\varepsilon2}\frac{\varepsilon^2}{k} \tag{13}$$

Transport equation for the thermal flux can be written by

$$\frac{\partial}{\partial x_k}(U_k\overline{u_i\theta})=D_{i\theta}+P_{i\theta}+\Phi_{i\theta}-\varepsilon_{i\theta} \tag{14}$$

where,

$$D_{i\theta}=-\frac{\partial}{\partial x_k}(\overline{u_iu_k\theta})$$

$$P_{i\theta}=-\left[\overline{u_iu_k}\frac{\partial T}{\partial x_k}+\overline{u_k\theta}\frac{\partial U_i}{\partial x_k}\right]$$

$$\Phi_{i\theta}=\overline{\frac{p}{\rho}\frac{\partial\theta}{\partial x_k}}$$

$$\varepsilon_{i\theta}=(a+\nu)\overline{\frac{\partial u_i}{\partial x_k}\frac{\partial\theta}{\partial x_k}}$$

Daly and Harlow's gradient model (1970) is adopted for the turbulent diffusion term, $D_{i\theta}$, as follows.

$$D_{i\theta}=\frac{\partial}{\partial x_k}\left[c_\theta\frac{k}{\varepsilon}\overline{u_ku_l}\frac{\partial\overline{u_i\theta}}{\partial x_l}\right] \tag{15}$$

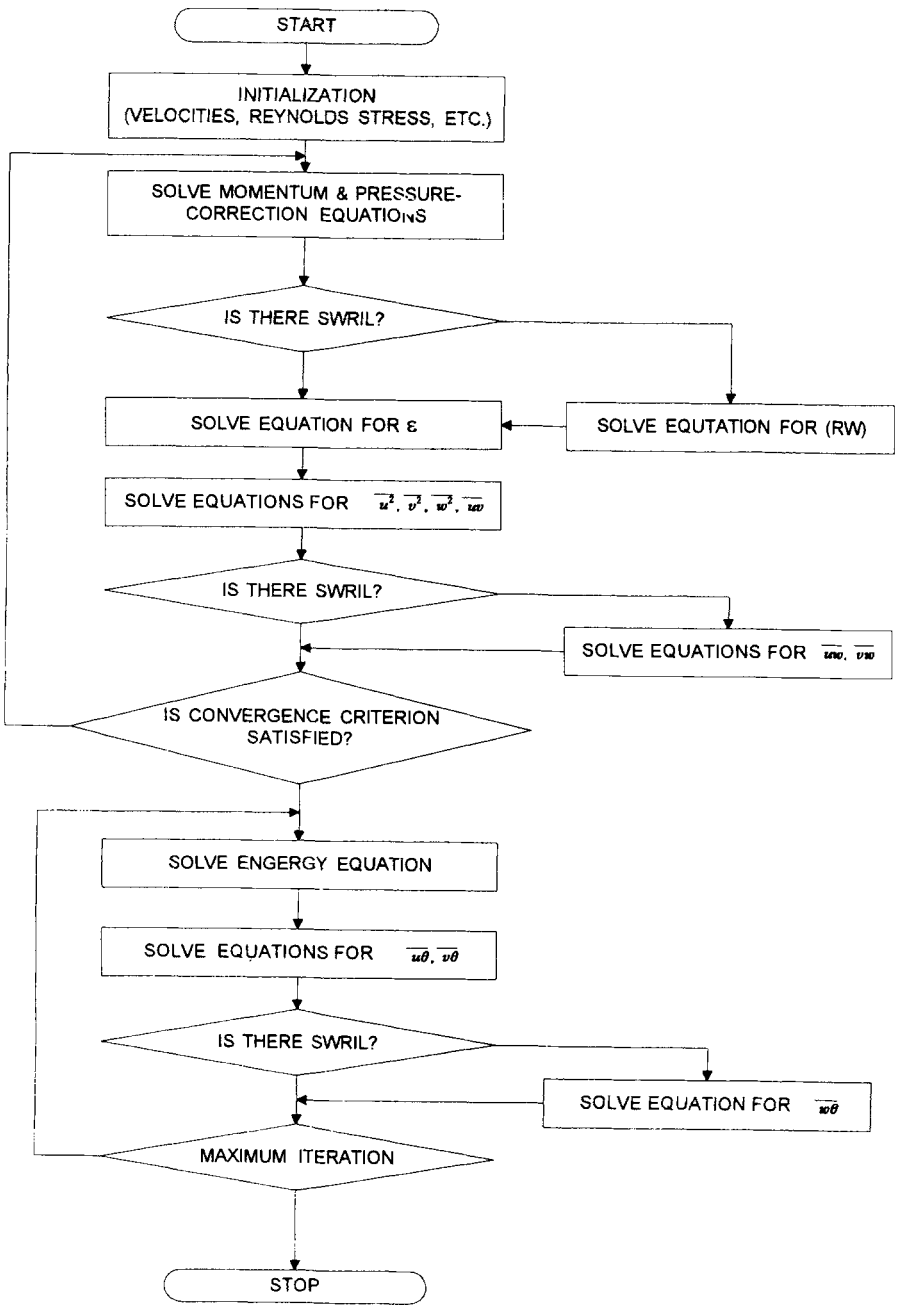

Fig. 1 Flow chart of computational procedure

Table 1 Model constant

$C_.$	C_2	C_1'	C_2'	$C_{\varepsilon 1}$	$C_{\varepsilon 2}$	$C_{1\theta}$	$C_{2\theta}$	C_S
1.8	0.6	0.5	0.3	1.44	1.92	3.0	0.5	0.22
C_c	C_θ	C_μ	C_f	χ	E	Pr	Pr_t	
0.18	0.11	0.09	9.24	0.4187	9.723	5.12	0.9	

As for the dissipation term, $\varepsilon_{i\theta}$, it is assumed that turbulence is isotropic in high-Reynolds -number flows, and consequently it is zero because there is no isotropic first-order tensor.

To the pressure-scrambling term, $\Phi_{i\theta}$, there are three different contributions, which are due to turbulent motion ($\Phi_{i\theta,1}$), mean motion ($\Phi_{i\theta,2}$), and wall reflection ($\Phi_{i\theta,w}$).

$$\Phi_{i\theta}=\Phi_{i\theta,1}+\Phi_{i\theta,2}+\Phi_{i\theta,w} \tag{16}$$

As a model for $\Phi_{i\theta,1}$, Monin's popular model (1965) is adopted in this work as follows.

$$\Phi_{i\theta,1}=-c_{1\theta}\frac{\varepsilon}{k}\overline{u_i\theta} \tag{17}$$

The destruction of production model (Launder, 1976) which is used for $\Phi_{i\theta,2}$ is written as

$$\Phi_{i\theta,2}=c_{2\theta}\overline{u_k\theta}\frac{\partial U_i}{\partial x_k} \tag{18}$$

The effects of wall reflection are assumed to be small unlike the case in stress equation. Thus, the corresponding term is neglected in this work.

The governing equations are discretized by finite volume method with power-law scheme. And, the solution procedure is based on SIMPLE algorithm (Patankar, 1980). The flowchart of computational procedure is shown in Fig. 1.

At the inlet to the computational domain, which coincides with the plane of expansion, axial and tangential components of velocity and turbulent normal stresses are given by the experimental data (Dellenback, 1986). And, the dissipation rates are assumed as $\varepsilon=c_\mu\frac{k^{\frac{2}{3}}}{0.01D}$. Turbulent shear stresses at the inlet are computed from the constitutive relations using $k-\varepsilon$ model.

At the exit, streamwise gradients of all variables are neglected. The wall functions adopted in the near-wall region are as follows.

$$\frac{U_p}{(\frac{\tau}{\rho})_w}c_\mu^{\frac{1}{4}}k_p^{\frac{1}{2}}=\frac{1}{\chi}\ln\left[\frac{Ey_p\ (c_\mu^{\frac{1}{2}}k_p)^{\frac{1}{2}}}{\nu}\right] \tag{19}$$

$$\frac{T_w-T_p}{q_w''}\rho c_p c_\mu^{\frac{1}{4}}k_p^{\frac{1}{2}}=\frac{Pr_t}{\chi}\cdot\ln\left[\frac{Ey_p\ (c_\mu^{\frac{1}{2}}k_p)^{\frac{1}{2}}}{\nu}\right]+P_f \tag{20}$$

where P_f is obtained from the following equation (Habib and McEligot, 1982).

$$P_f=c_f\left(\frac{Pr}{Pr_t}-1\right)\left(\frac{Pr_t}{Pr}\right)^{\frac{1}{4}} \tag{21}$$

The model constants used in this work are listed in Table 1.

3. Results and Discussion

In this work, the flows through an sudden expansion in a circular pipe with and without swirl are numerically analyzed to obtain the characteristics of convective heat transfer. The results with Reynolds stress model are compared with the experimental data of Dellenback (1986), which were obtained under uniform wall heat flux condition.

The swirl number which measures the relative strength of the swirl is defined as follows,

$$S=\frac{\int_0^R r^2UWdr}{R\int_0^R rU^2dr} \tag{22}$$

where R is a radius of the pipe. The flows are calculated at two swirl numbers, 0.17 and 0.74. The latter corresponds to the strong swirl which causes the recirculation around the axis as shown in the experiment of Dellenback (1986). Reynolds number in upstream tube is commonly 100, 000. And, the diameter ratio of the expansion is 0. 5.

The length of computatonal domain obtained

from preliminary test is 30D where D is a diameter of the downstream tube. Hogg and Leschziner (1989) as well as Jones and Pascau (1989) have specified axial velocity profile as an exit boundary condition, to stabilize the numerical solutions. However, in these calculations, we could obtain the converged solutions with Neumann conditions which neglect the axial gradients at the exit. From the grid-dependency test, the grid of 52×48 shown in Fig. 2 is employed.

The results for the flowfield as well as those of preliminary tests are reported by Kim and Chang (1996) in detail. In this report, the computational results of mean velocity and turbulent stresses without swirl show relatively good agreements with experimental data. However, in the prediction of axial velocity, the results of the strongly swirling flow ($S=0.74$) show large discrepancies in the wall-bounded recirculation zone, but exhibiting good agreements downstream. In the case of a tangential velocity profile, the discrepancies are not so severe as in the axial velocity profile. However, compared with experimental data, the results show that the tangential velocity decays rapidly near the wall, but, slowly near the axis. The Reynolds stress model gives generally good results for the turbulence intensities. The results just downstream of the expansion are better than those without swirl.

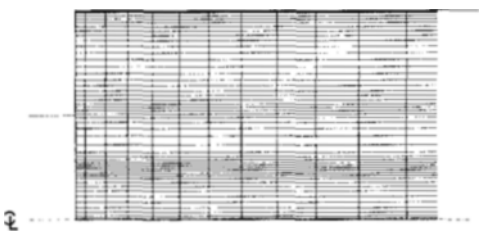

Fig. 2 Grid system (inlet part)

Figure 3 shows the computational results for the streamlines in three different flowfields with and without swirl. In the case with no swirl, we can find a relatively large recirculation zone, and also the secondary vortex in the corner of the expansion. When swirl is imposed on the flow, the secondary vortex disappears, and the wall-bounded recirculation zone shrinks smaller as swirl number increases. In the case of a strong swirl ($S=0.74$), a large on-axis recirculation zone is found, and thus the streamline pattern is much different from that with weak swirl ($S=0.17$).

Contours of constant turbulent kinetic energy based on the computational results are shown in Fig. 4. When a weak swirl is introduced in the

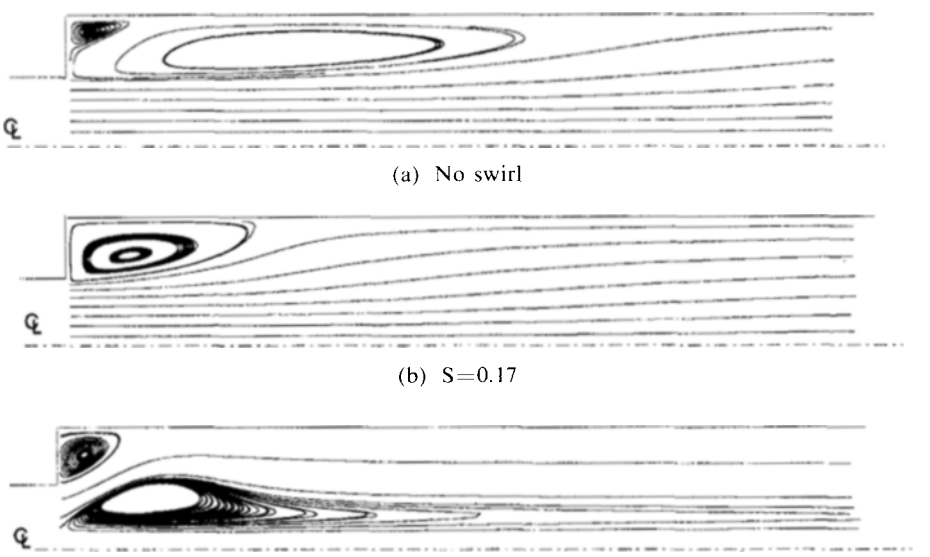

(a) No swirl

(b) S=0.17

(c) S=0.74

Fig. 3 Streamlines (Re=100,000)

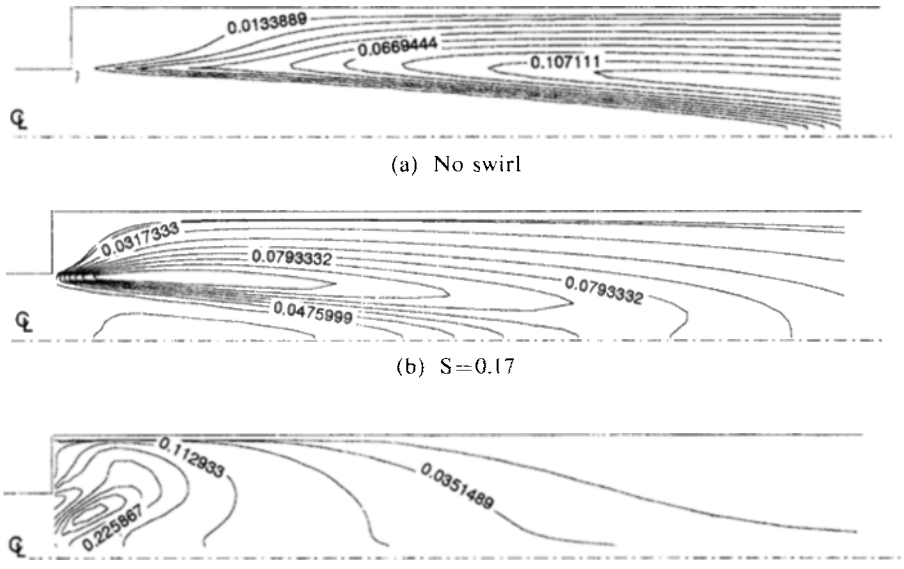

(a) No swirl

(b) S=0.17

(c) S=0.74

Fig. 4 Turbulent kinetic energy contours (Re=100,000)

flow, the swirl enhances the diffusion in radial direction. However, the on-axis recirculation induced by the strong swirl changes the entire structure of the turbulence field with large production of turbulent kinetic energy near the axis.

For the flow without swirl, wall temperature distributions and local Nusselt numbers normalized by an effective Nusselt number for the fully developed pipe flow, are compared in Figs. 5 and 6, respectively. The fully developed Nusselt numbers used for the normalization were obtained by Dittus-Boelter correlation for computational results and by Sieder-Tate correlation for experimental data. Thus, this can present problems for comparison of the results. If the experimental data had been normalized using the Dittus-Boelter relation rather than the Sieder-Tate correlation, then peak values of Nu/Nu_{fd} would have been 8% larger than the value shown in the figure as mentioned by Dellenback (1986). However, such amount of difference dose not seem to affect the qualitative comparisions of the present results. In Figs. 5 and 6, large discrepancies are found between computational results and experimental data. The bendings of computational profile near the inlet are caused by the secondary vortex. The maximum heat transfer rate is underestimated in

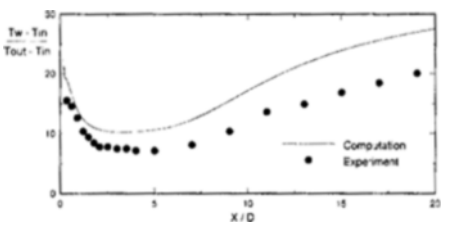

Fig. 5 Wall temperature distributions (no swirl case)

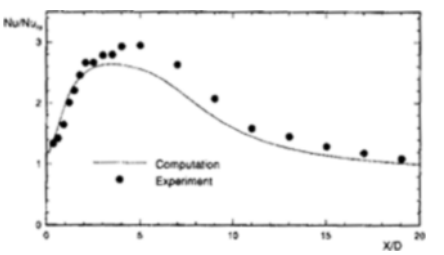

Fig. 6 Local Nusselt number distributions (no swirl case)

this calculation. And, the location of this maximum heat transfer rate is shifted to the inlet by about one and a half x/D by the computation.

In the case with weak swirl (Figs. 7 and 8), the discrepancy in maximum heat transfer rate becomes larger. The experimental data indicate

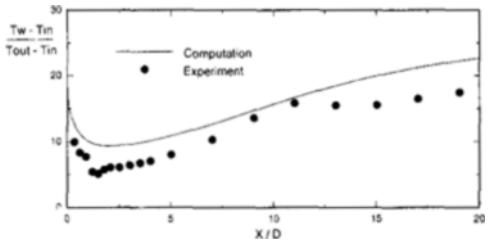

Fig. 7 Wall temperature distributions (S=0.17)

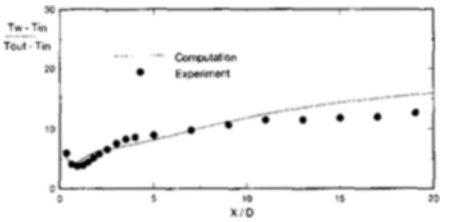

Fig. 9 Wall temperature distributions (S=0.74)

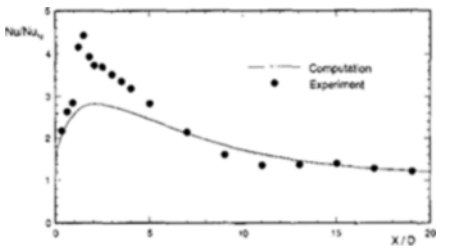

Fig. 8 Local Nusselt number distributions (S=0.17)

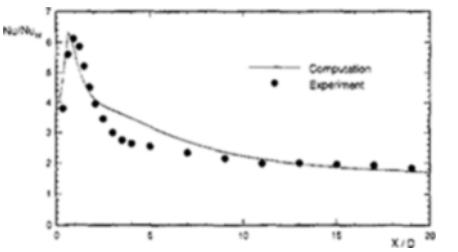

Fig. 10 Local Nusselt number distributions (S=0.74)

that the heat transfer rates in the wall-bounded recirculation zone are enhanced largely by the effects of the swirl. The computed heat transfer rates however, do not show the full effects of the swirl. On the other hand, in the case of a strong swirl shown in Figs. 9 and 10, the results are much different. The Reynolds stress model predicts the maximum heat transfer rate almost same as the empirical measurement. The computed Nusselt numbers show better agreements with experimental data downstream of $x/D=10$ in both weak and strong swirl cases than those without swirl. And, predictions for the location of maximum Nusselt number are also relatively accurate in these cases of swirl.

According to the experimental data, the maximum Nusselt number increases consistently in magnitude and move upstream with increasing swirl number. This upstream migration results from the shortening of the reattechment length, which causes shear rates and hence production of turbulent kinetic energy to increase with consequently higher heat transfer rates.

As discussed by Launder (1984), the use of conventional wall function usually results in the predictions of lower maximum Nusselt number than the experimental data. Thus, he recommends to use the low-Reynolds-number version of turbulence closure in the predictions of convective heat transfer. However, the present results for the strongly swirling flow are not consistent with the above mentioned general trend. This seems to be concerned with the formation of an on-axis recirculation zone, and also with the fact that the Reynolds stress model does not take account for the full effects of weak streamline curvature. In the computation, the large production of turbulent kinetic energy due to the strong effects of streamline curvature in the on-axis recirculation zone enhances the maximum heat transfer rate up to the measurement.

4. Conclusion

The Reynolds stress turbulence closure used in this work to predict the heat transfer in the flows with and without swirl downstream of an abrupt pipe expansion, regenerates the characteristics of the flows, such as secondary corner vortex in non-swirl case, and on-axis recirculation zone extended far downstream in the case with strong swirl. However, the results compared with experimental data indicate that the effects of swirl on heat transfer rate are not fully accounted for the

case with weak swirl, but also indicate that the strong swirl causing the on-axis recirculation increases the maximum heat transfer rate in wall-bounded recirculation zone up to the valve almost same as the experimental measurement, which can be considered as an overestimation taking into account that the logarithmic wall function generally underestimates the heat transfer rate.

Acknowledgement

The authors wish their gratitude to Inha University and KOSEF(94-0200-06-3) for the financial supports to this study.

References

Daly, B. J. and Harlow, F. H., 1970, "Transfer Equations in Turbulence," *Phys. Fluids*, Vol. 13, p. 2634.

Dellenback, P. A., 1986, "Heat Transfer and Velocity Measurements in Turbulent Swirling Flows Through An Abrupt Axisymmetric Expansion," PhD thesis, Arizona State Univ.

Dellenback, P. A., 1987, "Heat Transfer to Tubulent Swirling Through A Sudden Axisymmetric Expansion,"*J. of Heat Transfer*, Vol. 109, pp. 613~620.

Gibson, M. M. and Launder, B. E., 1978, "Ground Effects on Pressure Fluctations in the Atmospheric Boundary Layer," *J. of Fluid Mech.*, Vol. 86, pp. 491~511.

Habib, M. A. and McEligot, D. M., 1982, "Turbulent Heat Transfer in Swirl Flow Downsteam of an Abrupt Pipe Expansion," *Proc. of the 7th Int. Heat Transfer Conf.*, Washington, D. C., pp. 159~165.

Hogg, S. and Leschziner, M. A., 1989, "Computation of Highly Swirling Confined Flow with a Reynolds Stress Turbulence Model," *AIAA J.*, Vol. 27, 1989, pp. 57~63.

Jackson, T. W. and Lilley, D. G., 1983, "Single-Wire Swirl Flow Turbulence Measurements," *AIAA Paper* 83-1202.

Jones, W. P. and Pascau, A., 1989, "Computation of Confined Swirling Flows with a Second Moment Closure," *ASME Trans., J. of Fluids Eng.*, pp. 248~255.

Kim, K. Y. and Chang, Y. S., 1996, "Prediction of Strongly Swirling Turbulent Flow Downstream of an Abrupt Pipe Expansion," *Advances in Turbulence Research-1996*, Seoul, pp. 99~108 (also to be published in *Korean J. of Air-Conditioning and Refrigeration Engineering*).

Kim, K. Y. and Lee, Y. J., 1994, "Prediction of Turbulent Heat Transfer Downstream of an Abrupt Pipe Expansion," *KSME J.*, Vol. 8, pp. 248~254.

Launder, B. E., Reece, G. J. and Rodi, W., 1975, "Progress in the Development of Reynolds-Stress Turbulence Closure," *J. of Fluid Mech.*, Vol. 68, pp. 537~566.

Launder, B. E., 1976, Turbulence (Edited by P. Bradshow), Springr, Berlin, pp. 232~287.

Launder, B. E., 1984, "Numerical Computation of Convective Heat Transfer in Complex Turbulent Flows," *International J. of Heat and Mass Transfer*, Vol. 27, pp. 1485~1491.

Monin, A. S., 1965, "On the Symmetry of Turbulence in the Surface Layer of Air," *IZV Atm. Oceanic Phys.*, Vol. 1, pp. 45~54.

Partankar, S. V., 1980, *Numerical Heat and Transfer and Fluid Flow*, McGraw-Hill.

Prud'homme, M. and Elghobashi, S., 1986, "Turbulent Heat Transfer near The Reattatchment of Flow Downstream of a Sudden Pipe Expansion," *Numerical Heat Transfer*, Vol. 10, pp. 349~368.

Rhode, D. L., Lilley, D. G. and McLaughlin, D. K., 1983, "Mean Flowfields in Axisymmetric Combuster Geometries with Swirl," *AIAA J.*, Vol. 21, pp. 593~600.

Rotta, J., 1951, "Statistische Theorie Night homogener Turbulenz," *Z. Phys*, Vol. 129, pp. 547~573.

Sultanian, B. K., 1984, "Numerical Modeling of Turbulent Swirling Flow Downstream of an Abrupt Pipe Expansion," PhD thesis, Arizona State Univ.

Yoon, H. K. and Lilley, D. G., 1984, "Five-Hole Pitot Time-Mean Velocity Measurements in Confined Swirling Flows," *AIAA J.*, Vol. 22, pp. 514~515.